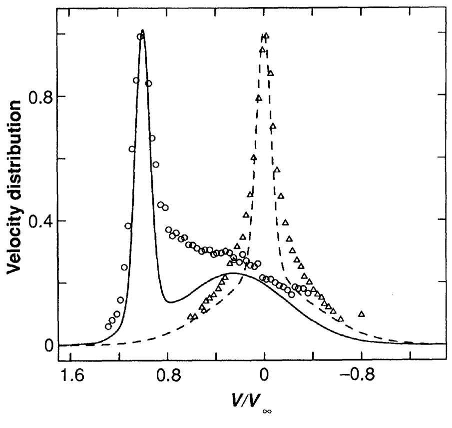

Fig. 3. Mott-Smith distribution and experiment ($\bar{n}$ = 0.285), illustrating failure to account for scattered molecules. Refer to Fig. 2a for DSMC technique comparison to the same results.

tions in Fig. 2 exhibit qualitatively unmistakable bimodal forms that have not been observed directly in any other study. Such a form was originally hypothesized by Mott-Smith (7). The distributions predicted by the DSMC technique are quantitatively representative of the observed distributions. On the other hand, there is an obvious quantitative difference between the observations and the Mott-Smith distribution in Fig. 3, which is caused by the presence in the experimental results of a large population of scattered molecules with velocities intermediate between those of the upstream and those of the downstream equilibrium distributions. The comparison shown in Fig. 3 is typical of the quantitative relationship between the experiments and the Mott-Smith distributions for all of the positions in the shock for which data are available. Predictions of the shock wave distribution functions from numerical solutions of the Boltzmann equation due to Yen and Ng (19) also exhibit a bimodal structure that, although not directly comparable to the M = 25 results, appears qualitatively similar to the distributions measured in the experiments.

We believe that the distribution function measurements described here show that for monatomic gas flows with only elastic binary collisions, the DSMC technique provides an accurate quantitative prediction of the molecular motion in highly nonequilibrium gas flows. Because the scattered component of the molecular motion was particularly well isolated by the extreme simplification of the upstream distribution function, the quantitative agreement between experiment and prediction represents an important, detailed test of the prediction technique.

REFERENCES AND NOTES

1. S. Chapman, *Philos. Trans. R. Soc. London Ser. A* **216**, 279 (1916).
2. H. W. Liepmann, R. Narasimha, M. T. Chahine, *Phys. Fluids* **5** (no. 11), 1313 (1962).
3. D. J. Evans and W. G. Hoover, *Annu. Rev. Fluid Mech.* **18**, 243 (1986).
4. H. Alsmeyer, *J. Fluid Mech.* **74**, 497 (1976).
5. R. E. Smalley, L. Wharton, D. H. Levy, *J. Chem. Phys.* **63**, 4477 (1975).
6. G. A. Bird, *Annu. Rev. Fluid Mech.* **10**, 11 (1978).
7. H. M. Mott-Smith, *Phys. Rev.* **82**, 855 (1951).
8. B. L. Holian *et al.*, *Phys. Rev. A* **22**, 2793 (1980); B. L. Holian, *ibid.* **37**, 2562 (1988).
9. V. Yu. Klimenko and A. N. Dremin, *Sov. Phys. Dokl.* **24**, 984 (1980).
10. E. P. Muntz, *Annu. Rev. Fluid Mech.* **21**, 387 (1989).
11. ——— and L. M. Harnett, *Phys. Fluids* **12** (no. 10), 2027 (1969).
12. T. Holtz and E. P. Muntz, *ibid.* **26** (no. 9), 2425 (1983).
13. E. P. Muntz, *ibid.* **11** (no. 1), 64 (1968).
14. L. N. Harnett and E. P. Muntz, *ibid.* **15** (no. 4), 565 (1972).
15. E. P. Muntz, *The Electron Beam Fluorescence Technique* (Advisory Group for Aerospace Research and Development AGARDograph 132, Neuilly-sur-Seine, France, 1969 (copies available from Clearinghouse for Federal Scientific and Technical Information, Springfield, VA).
16. D. Erwin and G. Pham-Van-Diep, in *Rarefied Gas Dynamics*, E. P. Muntz, D. Campbell, D. Weaver, Eds. (American Institute of Aeronautics and Astronautics, Washington, DC, in press).
17. G. A. Bird, *ibid.*
18. G. C. Maitland, M. Rigby, E. B. Smith, W. A. Wakeham, *Intermolecular Forces* (Clarendon, Oxford, 1981).
19. S. M. Yen and W. Ng, *J. Fluid Mech.* **65**, 127 (1974).
20. The unpublished data reported here were obtained in December 1966 with the assistance of L. Harnett and A. Dichter. The cooperation of L. Talbot and his colleagues at the University of California, Berkeley, was essential. S. Abel and B. Miller reduced all of the data. J. F. Muntz set up a real-time data transmission system between Berkeley and Philadelphia and helped with the experiments. The experimental work was supported by the Air Force Office of Scientific Research, contract AF 49(638)1526. The more recent analysis was supported by a National Aeronautics and Space Administration–Department of Defense Hypersonic Training and Research grant, NASA NAGW-1061.

13 March 1989; accepted 9 June 1989

Synthesis of Organic Salts with Large Second-Order Optical Nonlinearities

SETH R. MARDER, JOSEPH W. PERRY, WILLIAM P. SCHAEFER

A series of organic salts, in which the cation has been designed to have a large molecular hyperpolarizability, has been prepared. Variation of the counterion (anion) in many cases leads to materials with large powder second harmonic generation efficiencies, the highest of which is roughly 1000 times that of a urea reference.

THE DESIRE TO UTILIZE NONLINEAR optical (NLO) properties of materials in applications such as telecommunications, optical data storage, and optical information processing has created a need for new materials with very large second-order susceptibilities [$\chi^{(2)}$] (1–3). It is well established that π donor-acceptor compounds with their large differences between ground-state and excited-state dipole moments as well as large transition dipole moments can exhibit large molecular second-order optical nonlinearities (4). It is imperative that the nonlinear molecules reside in a noncentrosymmetric environment if the molecular hyperpolarizability (β) is to lead to an observable bulk effect [$\chi^{(2)}$]. Roughly 75% of all organic molecules crystallize in centrosymmetric space groups, leading to materials with vanishing $\chi^{(2)}$ (5). Strategies used to overcome this major obstacle include the use of chiral molecules (6), the incorporation of functional groups that encourage asymmetric intermolecular hydrogen bonding (6, 7), the synthesis of molecules with very small ground-state dipole moments but larger excited-state dipole moments (8), and the incorporation of the chromophore into organic (9) and inorganic hosts (10). In addition to these approaches, it is possible to orient the NLO active molecule in a glassy polymer matrix (11).

We present evidence that variation of counterions in organic salts is a simple and highly successful approach to creating materials with very large $\chi^{(2)}$. Meredith demonstrated that $(CH_3)_2NC_6H_4{-}CH{=}CH{-}C_5H_4N(CH_3)^+CH_3SO_4^-$ has a second harmonic generation (SHG) efficiency that is roughly 220 times that of urea (for a fundamental wavelength λ = 1907 nm) (12), which until recently (13) was the largest powder SHG efficiency reported. He suggested that in salts coulombic interactions could override the deleterious dipolar interactions that provide a strong driving force for centrosymmetric crystallization in covalent compounds (12). The use of ionic compounds further improves one's chances of achieving a noncentrosymmetric crystal structure because, in addition to the rationale described above, the counterions both separate and screen the dipolar chromophores from one another, thus reducing the

---

S. R. Marder and J. W. Perry, Jet Propulsion Laboratory, California Institute of Technology, Pasadena, CA 91109. W. P. Schaefer, Division of Chemistry and Chemical Engineering, California Institute of Technology, Pasadena, CA 91125.

undesirable dipole-dipole interactions.

In studying the role of organometallic compounds in nonlinear optics (*14*), we have found that $(C_5H_5)Fe(C_5H_4)-CH=CH-C_5H_4N(CH_3)^+I^-$ has an SHG efficiency roughly 220 times that of urea (λ = 1907 nm) (*15*). Furthermore, we observed, as did Meredith (*12*), that the magnitude of the powder SHG signal was sensitive to the nature of the counterion. The large SHG efficiencies cited above and the ease of synthesis of many salts by counterion metathesis led us to study a series of organic salts to determine whether the perturbation of crystal structure by counterion variation would, in effect, allow one to modify the packing of a given organic chromophore in the crystal.

Accordingly, we synthesized a series of N-methyl-stilbazolium salts with various donor groups and various counterions. The compounds were characterized by proton nuclear magnetic resonance spectroscopy, ultraviolet-visible spectroscopy, and elemental analysis (*16*). We examined 43 compounds with ten different chromophores (including the ferrocenyl compounds) by a modification of the Kurtz powder technique (*17*). We determined the powder SHG efficiencies by using 1907-nm fundamental radiation (SH at 953.5 nm) to avoid absorption of the SH by the dark-colored salts. We obtained the 1907-nm light by Raman shifting (first Stokes line of H_2) the 1064-nm output of a Q-switched Nd:yttrium-aluminum-garnet laser. A dual beam system (a urea sample was used in the reference arm) was used to provide normalization of the SH signals for laser shot-to-shot fluctuations. Pulse energies were in the range of 100 to 500 μJ with spot sizes of 2 to 3 mm. The diffusely backscattered SH signals were collected and isolated with filters and a monochromator. We detected the SH signals by using photomultiplier tubes (Hamamatsu R406), whose outputs were amplified and integrated with 10-ns gate widths. Samples were unsized microcrystalline powders obtained by grinding. The broad distribution of particle sizes was estimated to span from about 40 to 150 μm. Given the typically uncharacterized particle sizes and the possibility of preferential orientation of particles in assembling the samples, the uncertainties in the measured efficiencies can be quite large, perhaps a factor of 2 or more.

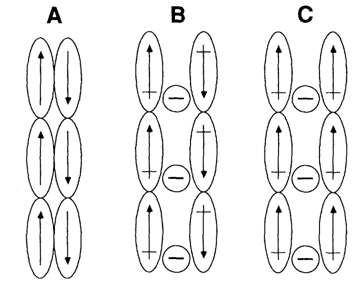

Fig. 1. Antiparallel arrangement of molecular dipoles typical for a covalent compound (**A**), antiparallel arrangement of molecular dipoles for a salt (**B**), and parallel arrangement of molecular dipoles for a salt (**C**).

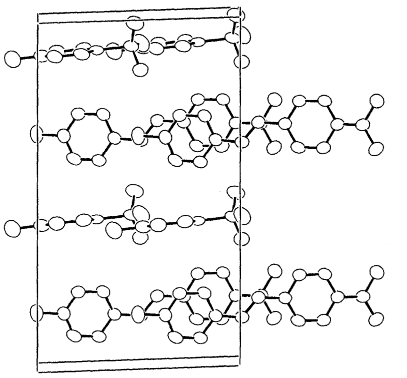

Fig. 2. Packing diagram for $(CH_3)_2NC_6H_4-CH=CH-C_5H_4N(CH_3)^+$ p-$CH_3C_6H_4SO_3^-$ viewed approximately along the *b* axis.

Table 1 summarizes the data for the counterions BF_4^-, $CF_3SO_3^-$, Cl^- (*18*), and p-$CH_3C_6H_4SO_3^-$. Many compounds in this series exhibit exceptionally large powder SHG efficiencies. For example, the yellow compound $CH_3OC_6H_4-CH=CH-C_5H_4N(CH_3)^+$ Cl^- exhibits an efficiency roughly 250 times that of the urea reference standard (λ = 1064 nm), $(CH_3)_2NC_6H_4-CH=CH-CH=CH-C_5H_4N(CH_3)^+CF_3SO_3^-$ has an efficiency 500 times that of the urea standard (λ = 1907 nm), and $(CH_3)_2NC_6H_4-CH=CH-C_5H_4N(CH_3)^+CH_3C_6H_4SO_3^-$ gave a signal 1000 times that of the urea standard (λ = 1907 nm). These data suggest that dipolar ionic compounds exhibit a higher tendency to crystallize noncentrosymmetrically than do dipolar covalent compounds. There were more compounds that exhibit SHG efficiencies more than 50 times that of urea than those that exhibited SHG values less than 0.05 times that of urea (Table 1). The versatility of the approach is further underscored by the observation that of the ten chromophores discussed here eight could be isolated with a counterion that gave rise to an SHG efficiency more than 35 times that of urea. Whereas in covalent molecules one might expect an antiparallel alignment of rows of dipolar chromophores, it is reasonable to suggest that the counterions in the compounds discussed here tend to align rows of the dipolar cations in a parallel manner so as to maximize the Madelung stabilization (Fig. 1). The above argument must be tempered by the caveat that the ultimate orientation of molecules in a crystal lattice is governed by a delicate balance of steric and multipolar effects.

Table 1. Summary of powder SHG efficiencies for compounds of the form $RCH=CHC_5H_4NCH_3^+X^-$. Values reported are SH intensities relative to that of a urea powder standard (50- to 100-μm particle size). The upper value given is for 1907-nm fundamental radiation, and the lower value is for 1064-nm fundamental radiation.

R	X^-			
	$CF_3SO_3^-$	BF_4^-	p-$CH_3C_6H_4SO_3^-$	Cl^-(*18*)
$4\text{-}CH_3OC_6H_4\text{-}$	50 54	0 0	120 100	60 270
$4\text{-}CH_3OC_6H_4\text{-}CH=CH\text{-}$	0 0	1.0 2.2	28 50	48 4.3
$4\text{-}CH_3SC_6H_4\text{-}$	0 0	0 0	 1	0 0
$2,4\text{-}(CH_3O)_2C_6H_3\text{-}$	40 67	5.5 2.9	0 0.08	0.4 0.7
$C_{10}H_8$-(pyrenyl)	0.8 1.1		37 14	
$4\text{-}(\overline{CH_2CH_2CH_2CH_2N})C_6H_4\text{-}$	0.5 0.06	5.2 0.05	0.2 0.03	1.1 0
$4\text{-}BrC_6H_4\text{-}$	0 0	0 0.02	1.7 5.0	22 100
$4\text{-}(CH_3)_2NC_6H_4\text{-}$	0 0	75,(*12*)	1000 15	0 0
$4\text{-}(CH_3)_2NC_6H_4\text{-}CH=CH\text{-}$	~500 5	350 4.2	115 5	0 0

In order to see if such alignments do occur in dipolar ionic crystals, we determined the crystal structure of $(CH_3)_2NC_6H_4-CH=CH-C_5H_4N(CH_3)^+$ p-$CH_3C_6H_4SO_3^-$ (*19*). This compound crystallizes in the monoclinic space group *Cc*. The basic structure illustrated in Fig. 2 is in accord with what one would predict on the basis of the reasoning described above. The anionic tosylate is situated close to the pyridinium moiety and in effect serves to line up adja-

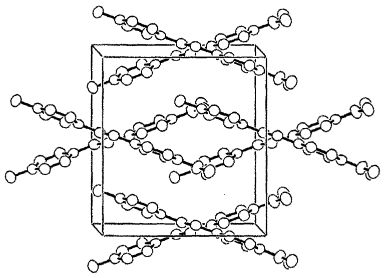

Fig. 3. Packing diagram for the same compound viewed approximately along the *c* axis (tosylate anions have been removed for clarity).

cent rows of cationic chromophores in a parallel manner (Figs. 2 and 3). The perpendicular distance between chromophores within a stack is about 3.4 Å, suggesting that the excellent alignment of the chromophores within a given row may be assisted by π-stacking. The only deviation from a completely aligned system is the 20° angle between the long axis of the molecules and the polar *a* axis of the crystal. In space group *Cc* the optimal angle for phase matching (*20*) is 35.3° between the charge-transfer axis of the nonlinear chromophore and the *b* axis of the crystal and, as such, the observed orientation is not well optimized for SHG, yet the powder efficiencies are large. In any case, given this excellent alignment in the crystal, extremely large electro-optic coefficients are expected (if the β_{zzz} is along the charge-transfer axis, then 83% of β_{zzz} is maintained along the polar *a* axis).

Our results demonstrate that the organic "salt methodology" can be used to obtain materials with very large $\chi^{(2)}$. Further, it has been shown that nonconventional donors such as Br^- and the pyrenyl moiety can be incorporated into molecules that, in the correct crystallographic environment, exhibit substantial bulk susceptibilities. We believe that this study represents an important step in decoupling the design of desirable molecular properties (large molecular nonlinearity and transparency) from the dipolar orientational requirements of $\chi^{(2)}$ materials. If the counterion is covalently linked to the ionic chromophore, then many of the desirable features of the "salt methodology" (large β and large dipole moment) can be used productively in an oriented polymer format.

REFERENCES AND NOTES

1. D. J. Williams, *Angew. Chem. Int. Ed. Engl.* **23**, 690 (1984).
2. D. J. Williams, Ed., *Nonlinear Optical Properties of Organic and Polymeric Materials* (ACS Symposium Series 233, American Chemical Society, Washington, DC, 1983).
3. D. S. Chemla and J. S. Zyss, Eds., *Nonlinear Optical Properties of Organic Molecules and Crystals* (Academic Press, Orlando, FL, 1987).
4. J. L. Oudar and D. S. Chemla, *J. Chem. Phys.* **66**, 2664 (1977); B. F. Levine and C. G. Bethea, *ibid.*, p. 1070; S. J. Lalama and A. F. Garito, *Phys. Rev. A* **20**, 1179 (1979).
5. J. F. Nicoud and R. W. Twieg, in (*3*), vol. 1, p. 242.
6. R. W. Twieg and K. Jain, in (*2*), p. 57.
7. J. S. Zyss, J. F. Nicoud, M. Koquillay, *J. Chem. Phys.* **81**, 4160 (1984).
8. J. S. Zyss *et al.*, *ibid.* **74**, 4800 (1981).
9. S. Tomaru *et al.*, *J. Chem. Soc. Chem. Commun.* **1984**, 1207 (1984); W. Tam *et al.*, *Chem. Mater.* **1**, 128 (1989); I. Weissbuch *et al.*, *ibid.*, p. 114.
10. S. D. Cox, T. E. Gier, J. D. Bierlein, G. D. Stucky, *J. Am. Chem. Soc.* **110**, 2986 (1989).
11. K. D. Singer, J. E. Sohn, S. J. Lalama, *Appl. Phys. Lett.* **49**, 248 (1986).
12. G. R. Meredith, in (*2*), p. 30.
13. W. Tam, Y. Wang, J. C. Calabrese, R. A. Clement, *Proc. Soc. Photo.-Opt. Instrum. Eng.* **971**, 107 (1988).
14. M. L. H. Green *et al.*, *Nature* **330**, 360 (1987).
15. S. R. Marder and J. W. Perry, in preparation.
16. Synthetic details will be described elsewhere: S. R. Marder *et al.*, in preparation.
17. S. K. Kurtz and T. T. Perry, *J. Appl. Phys.* **39**, 3798 (1968).
18. The Cl^- salts are hygroscopic, which is evidenced by elemental analysis, differential scanning calorimetry, and thermogravimetric analysis. We have not obtained satisfactory analysis for the Cl^- salts, although the agreement improves when calculated as some form of hydrate. Despite this, we can obtain reproducible SHG efficiencies, which are dependent on the degree of hydration.
19. $C_{23}H_{26}N_2SO_3$; molecular weight, 410.54; monoclinic, *Cc*(#9), $a = 10.365(3)$ Å, $b = 11.322(4)$ Å, $c = 17.893(4)$ Å, $\beta = 92.24(2)°$, $V = 2098.2(11)$ Å^3, $Z = 4$, where β is the crystallographic angle between *a* and *c*, *V* is the cell volume, and *Z* is the number of formula units per cell (figures in parentheses are the estimated standard deviations in the last figure). MoKα radiation, 3891 reflections collected, 1850 independent reflections used in full matrix least-squares refinement, for 1777 reflections with $F_o^2 > 0$; R ($\Sigma \mid F_o - \mid F_c \mid\mid / \Sigma F_o$, where F is the structure factor) = 0.033, goodness of fit ($[\Sigma w(F_o^2 - F_c^2)^2/(n - p)]^{1/2}$, where w is the weight of the reflection, n is the number of data, p is the number of parameters refined) = 1.81, and subscripts o and c refer to observed and calculated values, respectively. All nonhydrogens refined anisotropically. Hydrogen atom parameters were assigned from difference maps or by calculation with C–H = 0.95 Å.
20. J. S. Zyss and J. L. Oudar, *Phys. Rev. A* **26**, 2028 (1982).
21. This research was performed at the Jet Propulsion Laboratory (JPL), California Institute of Technology, as part of its Innovative Space Technology Center, which is supported by the Strategic Defense Initiative Organization through an agreement with the National Aeronautics and Space Administration (NASA). S.R.M. was supported by a NASA National Research Council Resident Research Associateship at JPL, and he thanks R. Grubbs for access to synthetic facilities. The diffractometer used in this study was purchased with a grant from the National Science Foundation. We thank B. G. Tiemann, P. Groves, and K. J. Perry for technical assistance.

3 April 1989; accepted 6 June 1989

Scandinavian, Siberian, and Arctic Ocean Glaciation: Effect of Holocene Atmospheric CO_2 Variations

D. R. LINDSTROM AND D. R. MACAYEAL

A computer model of coupled ice sheet–ice shelf behavior was used to evaluate whether observed changes in atmospheric CO_2 concentration could have caused the advance and retreat of Pleistocene ice sheets in the Eurasian Arctic. For CO_2 concentrations below a threshold of approximately 250 parts per million, an extensive marine-based ice sheet covering Scandinavia, the Barents, Kara, and East Siberian seas, and parts of the Arctic Ocean developed in the model simulations. In the simulations, climatic warming associated with the Holocene rise of atmospheric CO_2 was sufficient to collapse this widespread glaciation and restore present-day ice conditions.

ICE CORE RECORDS SUGGEST THAT Pleistocene glacial episodes are associated with significant depletion of CO_2 in the atmosphere (*1*). The effect of this depletion on atmospheric temperature and water transport may account for the intensity and global synchronization of the glacial response to orbital variations (*2, 3*). In an effort to test this hypothesis, we conducted computer simulations of ice-sheet behavior in the Eurasian Arctic under specific climatic conditions (*4*). We focused our study on the Eurasian Arctic because the grounding of ice on its broad continental shelves and the development of thick floating ice shelves offshore may have reorganized Arctic Ocean thermohaline circulation (*5*). Under present conditions, sea-ice formation in the shallow seas of the Eurasian Arctic produces brine-enriched waters that drain into the deep and intermediate levels of the Arctic Ocean. Grounded ice-sheet expansion across these seas under glacial conditions would thus alter the thermohaline circulation and density stratification of the Arctic Ocean and the Norwegian and Greenland seas. These oceanographic consequences of Eurasian glaciation could account for decreased North Atlantic deep water production rates during the last glacial maximum (LGM) (*6*).

Our model predicts the two-dimensional horizontal flow, mass balance, and three-dimensional temperature distribution of an ice sheet in response to specified atmospheric boundary conditions (surface accumula-

D. R. Lindstrom, Department of Geological Sciences (M/C 186), College of Liberal Arts and Sciences, University of Illinois at Chicago, Box 4348, Chicago, IL 60680.
D. R. MacAyeal, Department of Geophysical Sciences, University of Chicago, Chicago, IL 60637.